Solution-Processed, Surface-Engineered, Polycrystalline CdSe-SnSe Exhibiting Low Thermal Conductivity

Christine Fiedler[1], **Yu Liu**[1], **Maria Ibáñez**[1]

[1] Institute of Science and Technology Austria (ISTA)

Corresponding Author

Maria Ibáñez
mibanez@ist.ac.at

Citation

Fiedler, C., Liu, Y., Ibáñez, M. Solution-Processed, Surface-Engineered, Polycrystalline CdSe-SnSe Exhibiting Low Thermal Conductivity. *J. Vis. Exp.* (207), e66278, doi:10.3791/66278 (2024).

Date Published

May 17, 2024

DOI

10.3791/66278

URL

jove.com/video/66278

Abstract

In recent years, solution processes have gained considerable traction as a cost-effective and scalable method to produce high-performance thermoelectric materials. The process entails a series of critical steps: synthesis, purification, thermal treatments, and consolidation, each playing a pivotal role in determining performance, stability, and reproducibility. We have noticed a need for more comprehensive details for each of the described steps in most published works. Recognizing the significance of detailed synthetic protocols, we describe here the approach used to synthesize and characterize one of the highest-performing polycrystalline *p*-type SnSe. In particular, we report the synthesis of SnSe particles in water and the subsequent surface treatment with CdSe molecular complexes that yields CdSe-SnSe nanocomposites upon consolidation. Moreover, the surface treatment inhibits grain growth through Zenner pinning of secondary phase CdSe nanoparticles and enhances defect formation at different length scales. The enhanced complexity in the CdSe-SnSe nanocomposite microstructure with respect to SnSe promotes phonon scattering and thereby significantly reduces the thermal conductivity. Such surface engineering provides opportunities in solution processing for introducing and controlling defects, making it possible to optimize the transport properties and attain a high thermoelectric figure of merit.

Introduction

Thermoelectric (TE) materials, which convert heat into electricity and *vice versa*, can play an important role in sustainable energy management[1]. However, the low conversion efficiencies combined with the relatively high production costs of these materials have limited their broad application for industrial and domestic use. To overcome present challenges, cost-effective synthetic methods and the use of abundant and non-toxic materials with significantly improved efficiency must be implemented.

The thermoelectric figure of merit $zT = S^2\sigma T/\kappa$, where S is the Seebeck coefficient, σ the electrical conductivity, T the absolute temperature, and κ the thermal conductivity,

determines the efficiency of these materials. Due to the strong coupling of these properties, maximizing *zT* is a challenge. It often entails tuning the electronic band structure and microstructural defects to control charge and phonon scattering mechanisms[2,3,4,5].

In the last decade, tin selenide (SnSe) has been explored as a non-toxic thermoelectric material due to its outstanding performance in its single crystal form (*zT:* *p*-type ~2.6, *n*-type ~2.8)[6,7]. However, single crystals are expensive to produce, limiting their applicability to devices. Alternatively, polycrystalline SnSe is cheaper to produce and mechanically more stable. The problem is that attaining high performance presents difficulties due to partial loss of anisotropy, diminishing electrical conductivity, greater ease of oxidation, and imprecise control of the doping level[8,9,10].

Polycrystalline inorganic TE materials are usually processed in two steps: preparation of the semiconductor in powder form followed by consolidation of the powder into a dense pellet. Powders can be prepared through high-temperature reactions and grinding or directly by ball-milling[11,12,13,14,15,16]. Alternatively, powders can be synthesized *via* solution methods (e.g., hydrothermal, solvothermal, aqueous synthesis), requiring less demanding conditions (i.e., lower reagent purity, lower temperatures, and shorter reaction times)[17,18,19,20,21].

This paper describes a method to produce dense SnSe nanocomposites from surface-modified SnSe particles that are synthesized in water. The process commences from the aqueous synthesis of SnSe particles, where reducing agents and bases are used to solubilize the Se and Sn reagents, respectively. When the solutions are combined, SnSe particles immediately start precipitating. After purification, SnSe particles are then functionalized with CdSe molecular complexes. During the annealing process, the molecular complexes decompose; forming CdSe nanoparticles[19]. The presence of CdSe nanoparticles inhibits grain growth and promotes the formation of many defects at varying length scales. These scattering sources result in low thermal conductivity and a high thermoelectric figure of merit[22].

Protocol

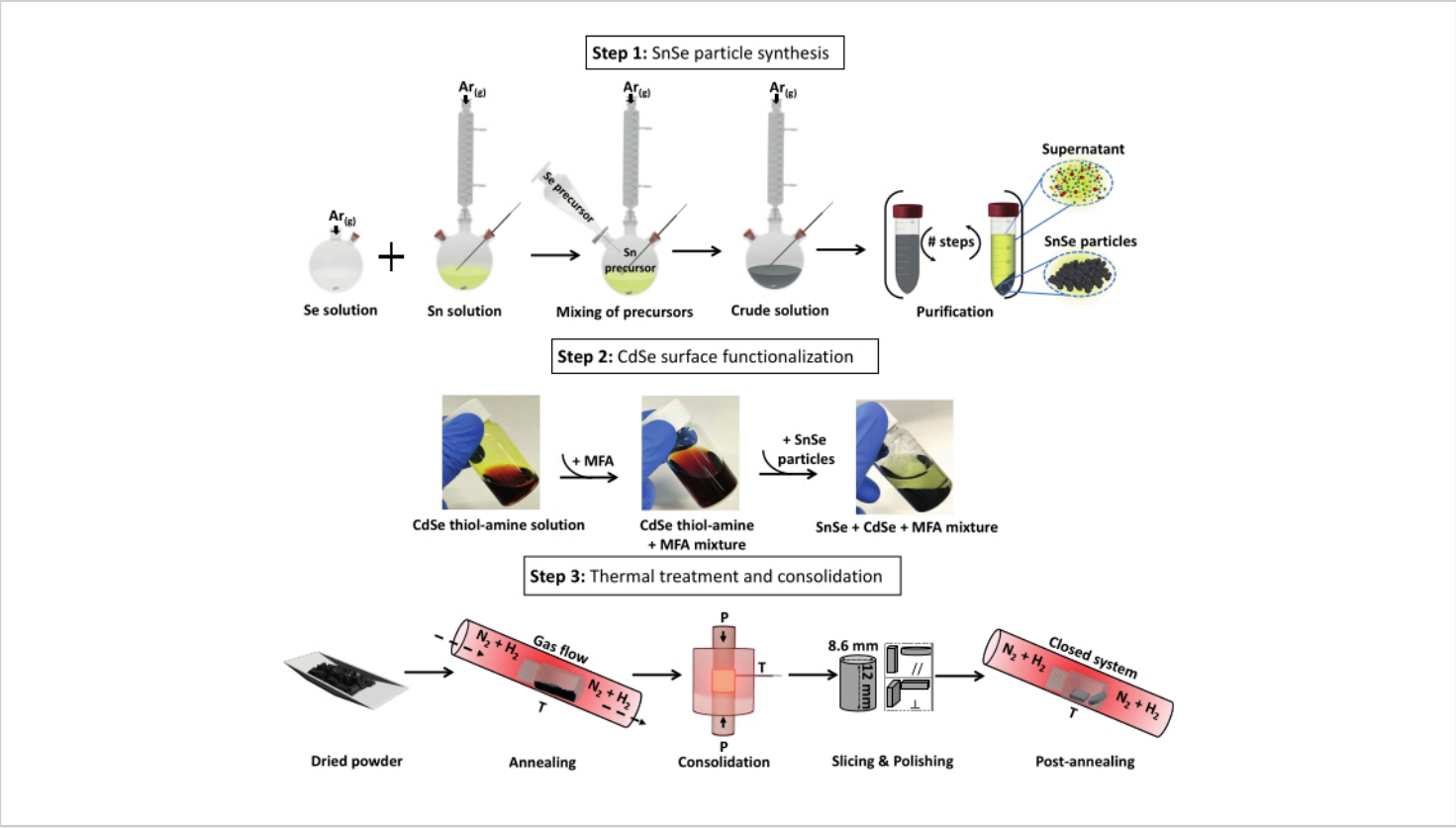

Figure 1: Steps for the production of CdSe-SnSe pellets divided into three steps: 1) SnSe particle synthesis, 2) particle surface functionalization with CdSe, and 3) thermal processing into dense CdSe-SnSe pellets. Abbreviation: MFA = *N*-methylformamide. Please click here to view a larger version of this figure.

1. Aqueous synthesis of SnSe particles

NOTE: SnSe particles are obtained through a co-precipitation reaction by mixing previously prepared Sn and Se precursors. After the particles are formed, a purification step is necessary to separate them from reaction byproducts and impurities.

1. Preparation of the Se precursor
    1. In a 500 mL two-neck round-bottom flask (one big and small neck) equipped with a stir bar, add 400 mL of deionized water using a measuring cylinder and start stirring. Weigh 6.05 g (160 mmol) of sodium borohydride powder (99% $NaBH_4$) in a weighing boat and add to the round-bottom flask through the big neck of the flask. Wait until complete dissolution, which is indicated when the solution turns transparent.
    2. Weigh 6.32 g (80 mmol) of selenium powder (≥99.5% Se) using weighing paper. Stop the stirring of the borohydride solution and slowly add the Se through the big neck of the flask.

NOTE: As hydrogen gas is produced during the dissolution, vigorous bubbling occurs (CAUTION: Hydrogen gas is flammable).

3. Once the bubbling has settled, place a rubber septum onto the small neck of the round-bottom flask. With a long tube attached from the Schleck line fitted with a connector, connect the flask to the Schleck line via the big neck of the flask under argon flow and restart stirring.

   NOTE: Grease all glassware joints before connecting to the Schlenk line to prevent the glassware from being lodged. The solution turns transparent with time under argon flow (~20 min), indicating dissolution of the Se.

2. Preparation of the Sn precursor

   1. In a 1000 mL three-neck round-bottom flask (one big neck in the center and two small necks) equipped with a stir bar, add 360 mL of deionized water using a measuring cylinder through the big neck of the flask. Place the flask into a heating mantle and then the mantle onto a stirring plate. Use one of the lateral necks of the flask to place an adapter with a thermocouple. Attach a condenser connected to the Schlenk line to the big neck, place a rubber stopper on the remaining neck of the flask, and commence stirring under argon flow.

   2. Remove the rubber septum, add 30.06 g (750 mmol) of sodium hydroxide pellets (≥98% NaOH), and place the septum back. Wait until the solution turns transparent upon complete dissolution (~5 min).

   3. Remove the septum again, add 16.25 g (72 mmol) of tin (II) chloride dihydrate powder (98% $SnCl_2 \cdot 2H_2O$), and place the septum back. Wait until the solution turns transparent with a yellow hue upon dissolution.

3. Mixing of the solutions; SnSe particle formation

   1. Set the Sn solution at 101 °C; once at this temperature, remove the septum and place a separating funnel. Allow argon to pass through the funnel for 5 min. Remove the rubber septum from the flask containing the Se solution and transfer the Se solution via the separating funnel to the Sn solution (flow rate 11 mL/s).

      NOTE: The solution will turn black immediately, indicating the formation of SnSe. (Total volume will be 760 mL)

   2. Once all the Se solution has been added, replace the funnel with a rubber septum, allow the mixture to reach the set temperature again (~101.0 °C), and continue stirring for an additional 2 h. Stop the heating, remove the heating mantel, and with the thermocouple still connected, place the round-bottom flask into a water bath while stirring.

4. Purification of particles

   1. Once the mixture is cooled to ~35 °C, disconnect the round-bottom flask from the Schleck line and place it onto a round-bottom flask support. Allow the particles to settle for 5 min and remove ~600 mL of supernatant via careful pouring. Divide the remaining crude solution among four centrifuge tubes, ~40 mL per tube. Centrifuge the crude solution at 4,950 × *g* for 1 min; this is washing #0; discard the supernatant.

      NOTE: The supernatant is yellow initially but changes to red on exposure to oxygen.

2. Add 40 mL of deionized water to each centrifuge tube with the precipitated particles and vortex the mixture for 1 min. Sonicate the mixture for 5 min in a sonicating bath and vortex for an additional 1 min before centrifuging (9,935 × *g* for 1 min). Discard the light yellow supernatant; this is washing #1).

3. Repeat step 1.4.2 but instead of water, use ethanol as the solvent; this is washing #2, 9,935 × *g* for 2 min). Purify additional 4x following step 1.4.2 alternating water (washings #3, 11,639 × *g* for 2 min and #5, 11,639 × *g* for 3 min) and ethanol (washings #4, 11,639 × *g* for 2 min and #6, 12,410 × *g* for 5 min).

   NOTE: With each washing, the supernatant becomes clear at washing #2 but becomes dark and turbid with the loss of particles.

4. After purification step #6, place the tubes in a desiccator under vacuum (>10 mbar) for at least 12 h to dry the powder. Transfer the tubes with the SnSe particles to a N_2-filled glovebox and use an agate mortar and pestle to obtain a fine powder. In one 20 mL vial, weigh 4.00 g of the resulting powder for further use in step 3.1. Store the remaining powder in another 20 mL vial inside the glovebox.

   NOTE: Following this instruction should result in ~14 g of material.

5. Reserve 20 mg of the powder for X-ray Diffraction (XRD) and Scanning Electron Microscopy (SEM) characterization (sample name: ***SnSe-Before Annealing***).

2. SnSe surface treatment with CdSe molecular complexes

1. Preparation of the CdSe molecular complexes

   1. In the glovebox, weigh 513.6 mg (4 mmol) of cadmium (II) oxide (≥99.98% CdO) and 316 mg (4 mmol) of selenium powder and place both powders in a 4 mL scintillation vial with a stir bar. Add 8 mL of ethylenediamine (99% $C_2H_8N_2$) and 0.8 mL of 1, 2-ethanedithiol (>95%, $C_2H_6S_2$), cap the vial, and stir until the mixture becomes translucent and reddish brown, indicating the formation of CdSe complexes upon the complete dissolution of CdO and Se (~20 min) as shown in **Figure 1**.

      NOTE: When handling solvents in the glovebox, turn off the blower and purge the system. This preserves the purification system.CAUTION: Thiols can shorten the life of the catalyst.

2. Surface treatment of SnSe particles

   1. Still within the glovebox, in a 20 mL scintillation vial with a stirring bar, add 10 mL of anhydrous *N*-methylformamide (vacuum-distilled, MFA) and 1.32 mL (0.6 mmol) of the CdSe molecular complexes prepared in step 2.1.1. Add this CdSe-MFA mixture to the 4.00 g of SnSe powder from step 1.4.4, cap the vial, and stir at room temperature for 48 h.

      NOTE: After this time, the supernatant changes color from red-brownish to yellow, indicating the adsorption of the CdSe complexes on the SnSe particle surface.

3. Purification of CdSe surface-treated SnSe particles

   1. Inside the glovebox, transfer the CdSe-SnSe mixture to a centrifuge tube and add 40 mL of

anhydrous ethanol (extra dry). Vortex the mixture for 1 min, centrifuge (12298 × *g* for 1 min), and discard the yellow supernatant.

2. Add 40 mL of anhydrous ethanol to the tube with the particles, vortex for 1 min, and centrifuge (12,298 × *g* for 1 min). Discard the supernatant, which is colorless.

3. Remove the tube with the powder from the glovebox and dry the particles under vacuum for a minimum of 12 h inside a desiccator (>10 mbar). Transfer the tube with the surface-treated particles back to the glovebox and use an agate mortar and pestle to obtain a fine powder. Store the resulting powder in a 20 mL vial in the glovebox for further use.
   NOTE: Following this instruction will result in ~4.00 g of material.

4. Reserve 20 mg of the powder for XRD and SEM characterizations (sample name: ***CdSe-SnSe-Before Annealing***).

3. Thermal treatments and consolidation

NOTE: To evaluate the effect of the surface treatment, we prepared samples with and without the CdSe complexes. The SnSe powders without the surface treatments are those obtained after step 1.1.3; the CdSe-SnSe powders are those obtained after step 2.3. In either case, to produce cylinders of 8.16 mm x 12 mm, we use approximately 4.00 g of SnSe and 4.00 g of CdSe-SnSe particles. From powders to dense pellets, both types of samples undergo the same processes as described in the following sections.

1. Annealing in a tubular furnace

   1. Remove the surface-treated powder from the glovebox.

   2. Open the gas in valve and gas out valve to allow forming gas (95% N_2 + 5% H_2, 0.3 L/min) to flow through the quartz tube of the tubular furnace for 5 min. Open one end of the tube, uncap the vial, and introduce the vial into the middle of the quartz tube, with the opening of the vial facing the direction of the gas flow. Seal the tube, and allow the forming gas to flow for an additional 10 min.

   3. Set the temperature profile of the furnace to heat to 500 °C at a heating rate of 10 °C/min and hold at this temperature for 1 h before cooling to room temperature naturally (~40 min). Run the program. Remove the powder from the furnace at room temperature and transfer it to the glovebox. Use an agate mortar and pestle to obtain a fine powder. Reserve 20 mg of the powder for XRD and SEM analysis (sample names: ***SnSe-After annealing*** and ***CdSe-SnSe-After annealing***)
      NOTE: Above 350 °C, there will be a red residue seen on the inside of the quartz tube of the furnace as Se evaporates and condenses on the cooler ends of the tube.

2. Consolidation by Spark Plasma Sintering (SPS), cutting, and polishing

   1. Loading of the die
      NOTE: See **Supplementary Table S1** for die characteristics: height: 60 mm, inner diameter: 8.6 mm, outer diameter: 30 mm, stem (x 2); 30 mm x 8 mm.

      1. Cut a piece of graphite sheet (thickness 0.254 mm) with the dimensions: 26 mm x 60 mm. Roll the graphite sheet and line the interior of the die.

Cut four discs out of the graphite sheet (Φ =8 mm).

2. Insert one stem halfway into the die, place two of the graphite discs so they sit flat on top of the stem, and press them by inserting the remaining stem and compressing the two stems together. Remove the last inserted stem and introduce the half-prepared die (remaining stem and the two graphite discs) into the glovebox.

3. Place the powder into the die using weighing paper and compress it with the other stem to compact the powder to create a flat surface. Remove the last inserted stem, place the remaining two graphite discs on top of the powder, and place the remaining stem (**Figure 2A**). Remove the die from the glovebox and compress the powder using a cold press (~0.3 kN) until the total height of the completed die is ~83 mm.

   NOTE: This step is required to fit the die into SPS (**Figure 2B**).

4. Open the SPS and place the prepared die in the center of the stage. Lower the upper electrode to fix the die in place and insert the thermocouple (see **Supplemental Figure S1** for details). Close the chamber, set the upper electrode **Z-axis control** to move **continuously down**, and apply vacuum.

5. After the manometer reaches its minimum, turn on the Pirani gauge, and wait 10 min. Choose the pressing conditions from the auto pattern table, applying an **axial pressure** of **47 MPa** at **500 °C** for **5 min** (**rate: 100 °C/min**). Set the **temperature** and **pressure controls** of the SPS to **auto**.

6. Check that the thermocouple is still inserted into the die, the **vacuum** is **<5 Pa**, the **pressure** and **temperature controls** are set to **automatic**, and the **upper electrode control** is set to **continuous-down**. In the wave logger software, commence with the measurement, track the pressure and Z-axis, and then press **sinter ON** to commence the consolidation.

   NOTE: Monitor the evolution of the parameters to ensure there are no fluctuations in current, voltage, Z-axis, or pressure while heating up.

7. Once the die has cooled to room temperature, turn off the vacuum and Pirani gauge, set **temperature** and **pressure** to **manual control**, and **Z-axis** to **stop-step**. Vent and open the chamber. Remove the thermocouple from the insert and raise the electrode to remove the die.

2. Cutting and polishing

   1. Remove the dense cylinder from the die by pushing the upper stem with a cold press, and then separate the cylinder from both stems using a snap-off blade.

   2. With an electric saw and the necessary adapters (see **Supplemental Figure S2** for adapter specifications), cut a pellet and a bar from the consolidated cylinder. Remove the graphite lining using a snap-off blade. Polish the samples evenly and smoothly with sandpaper (pellet: 1.3 mm thickness, 8 mm diameter; bar: 1.3 mm thickness, 7 mm height, 6.5 mm wide). Using a caliper, ensure the material dimensions

have been consistently achieved throughout the entirety of the samples. Store the bar and pellet in a 4 mL scintillation vial (sample names: ***SnSe bar and disc*** and ***CdSe-SnSe bar and disc***)

3. Post-annealing in forming gas
    1. Place the vial with the disc and bar into the quartz tube of the furnace, with the opening of the vial facing the direction of the gas flow. Allow the forming gas to flow for 10 min before closing the gas-out valve and gas-in valve to close the system.
    2. Set the temperature profile of the furnace to heat to **500 °C** at a heating rate of **10 °C/min** and hold at this temperature for **1 h**, allowing cooling to room temperature naturally (~40 min). Run the program.
    3. Once at room temperature, open the gas flow, then the valve in, and finally the valve out. Let gas flow for 5 min before opening the tube. Finally, open the tube, remove the vial, and stop the gas flow.
4. XRD measurements
    1. Preparation of powder samples for XRD
        1. Place 15 mg of the powders isolated for XRD measurements (samples: ***SnSe-Before Annealing***, ***CdSe-SnSe-Before annealing, SnSe-After Annealing,*** and ***CdSe-SnSe-After annealing***) into tubes, add 0.1-0.2 mL of ethanol into each tube, and sonicate for 30 s to disperse the powder in ethanol.
        2. Using a Pasteur pipette, transfer each powder onto a low background Si-sample holder, smoothly covering the entire holder, and let it dry.
    2. Preparation of bulk samples for XRD
        1. Apply a small piece of molding clay; make a pointed shape, in the center of the sample holder.
        2. Place the pellet/bar (samples: ***SnSe bar and disc*** and ***CdSe-SnSe bar and disc***) on top of the clay, and using a glass slide, press the sample until it is aligned with the side of the holder.

            NOTE: This ensures the pellet is placed at the proper height and ensures proper measurement of the diffraction angles with respect to the incident beam.
    3. XRD measurement of powders and pellets
        1. Measure all powders and pellets using the **experiment program** (**20-80°, resolution: 0.02°, scan rate: 1°/min**).
5. SEM characterization
    1. On an SEM stubble, place a strip of carbon tape and remove the protective seal.
        1. For powders, using the tip of the spatula, place ~1 mg of sample (i.e., before annealing or after annealing) onto the carbon tape.
        2. For pellets/bars, using a snap-off blade, cut a small piece of the sample and place it onto a new carbon tape on the stubble. Ensure that the inner part of the sample and not the surface is facing in the upward direction.
    2. Image the samples at x1K, x5K, x10K, and x20K magnification.

        NOTE: Always image a fresh cut of the samples for accurate representation, as oxidation can occur.

6. Seebeck coefficient (*S*) and Conductivity (*σ*) measurements in the LSR

NOTE: We perform temperature-dependent measurements to measure the Seebeck coefficient and resistivity while maintaining the set temperature. As SnSe is a layered compound and the polycrystalline sample shows a certain degree of texture, as can be seen by the XRD data, all pellets are measured in the direction parallel and perpendicular to the pressing axis. However, in the main text, only the results from the parallel direction are reported, as this direction shows the highest performance.

1. Loading the sample

1. Measure the dimensions of the sample (for the bar: thickness and width). In the measurement software, under the tab for data acquisition **DAQ**, introduce these **sample dimensions** and select the **sample shape**, **measurement file name** and **path**, and **sample description**.

2. Mount the sample between the electrodes, placing graphite paper (Φ = 0.13 mm) between the bar and electrodes and adjusting the knob until the bar is secure. Set the thermocouples (probes) in contact with the sample. Use a small stripe of graphite paper (Φ = 0.13 mm) to separate the bar from being in direct contact probes (see **Figure 3**). Adjust until the probes are in contact with the bar and then turn the knob for half a turn to ensure proper thermal contact.

NOTE: Applying too much force while adjusting the knob will lead to the breaking of the sample or bending during the heating cycle (plastic deformation). If the thermocouples are not pressed sufficiently, the Seebeck coefficient would be overestimated (**Figure 3**).

3. Check the contacts in the software from **Options/Test contacts**. Using the camera and associated software, measure the distance between the probes and input the **distance** into the software under **DAQ**.

NOTE: For the current sample dimensions, because a **maximum probe distance** of **4 mm** is set, the maximum distance recorded should not exceed this distance.

4. Place the Inconel susceptor (metal cover) over the sample carefully and insert the thermocouple. Close the furnace and apply vacuum for 10 min. Refill the chamber with helium and apply vacuum once more. Do this 3-4x to ensure that there is no air left in the system. Finally, refill with helium to a manometric pressure of ~+0.5 bar).

NOTE: The susceptor absorbs the infrared radiation of the furnace, heating the sample to the required temperature and avoiding contamination of the oven.

2. Measuring the resistance and Seebeck

1. Conduct another **contact test** to ensure good contact of the probes and electrodes with the sample and that there was no shift during the purging steps.

2. Conduct a **probe test** (I-V curve) to select the highest measuring current under which the samples show Ohmic behavior (20 mA).

3. Set the **temperature profile** within the software: **heating cycle, 30 °C to 500 °C and cooling rate, 500 °C to 30 °C at 20 °C/min** measuring **every 20 °C**. Run the measurements for three complete heating and cooling cycles.

7. Measuring the thermal diffusivity (*α*) in the LFA

1. Preparing the bulk samples

1. Polish the samples (***SnSe*** and ***CdSe-SnSe*** discs) to ~1 mm thickness. (disc: Φ =7.99 mm). Coat both sides of the two samples with graphite spray, which creates a smooth, non-reflective surface that will ensure the incident laser beam is not reflected and is efficiently transferred to the sample. Place the sample into the graphite sample holder (**Figure 4**). Open the analyzer, load the sample holder into the magazine, and close it.

2. Fill the liquid nitrogen reservoir to cool the detector. First, fill a small volume, wait until it settles, and then complete the rest. Apply vacuum on the analyzer chamber to avoid heat transfer by convection, which leads to an overestimation of the thermal diffusivity.
CAUTION: Pour liquid nitrogen slowly.

3. Introduce the **sample name** and **thickness** in the software **settings** and set the temperature profile from **30 °C** to **500 °C** at **50 °C/min**, measuring **every 50 °C** and turn on the **laser**. Carry out multiple (>3) measurements (**laser shot**) to ensure that the laser voltage, iris, amplifier, and acquisition time of the detector are adequate, which is represented by a good quality fit of >98%. Commence the **automatic** measurements.

4. Once the measurements are complete, turn off the laser, allow the chamber to cool to room temperature, vent the chamber, and remove the sample. Calculate the thermal conductivity using equation (**1**), where Cp is calculated heat capacity (Cp) using Dulong-Petite value and ρ is the density of the sample measured in instruction J.

$$\kappa = Cp \cdot \rho \cdot \alpha \quad (1)$$

8. Density measurement (Archimedes method)

NOTE: Density measurements are done after the transport measurements are finished.

1. Clean the pellet with ethanol to remove the graphite coating used for the thermal diffusivity measurements and polish it. Assemble the density measurement apparatus (see **Supplemental Figure S3**), ensuring no air bubbles are present within the water and tare the scale. Measure the temperature of the water.

2. Place the sample on top of the sinker and record the weight in air (m_{air}).

3. Place the sample in the water on the base of the sinker to record the weight in water (m_{water}).

4. Repeat steps 3.8.2 and 3.8.3 for 5x to have an average of the density. Using equation (**2**), calculate the density of the material.

$$\rho_{sample} = \frac{m_{air}}{m_{air} - m_{water}} \cdot \rho_{water}(T) \quad (2)$$

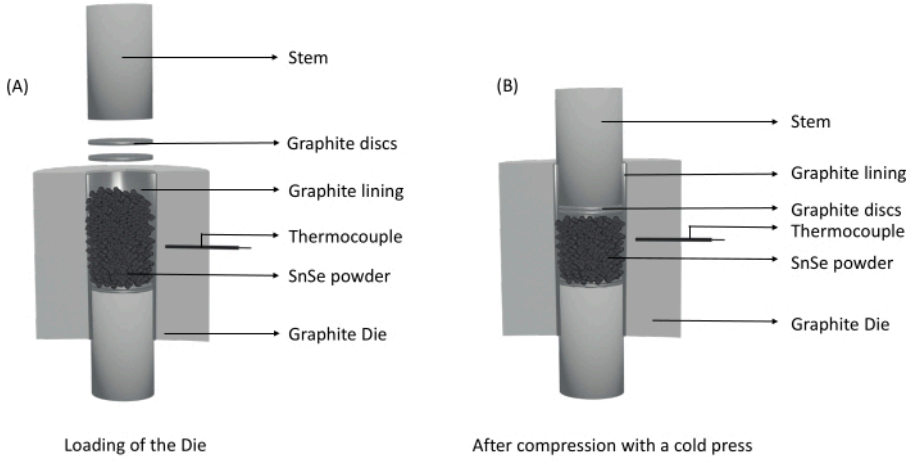

Figure 2: Illustrations of die preparation for consolidation. (**A**) Assembly of the graphite die with the powder. (**B**) After the powder is compressed using a cold press, the powder is compact, and the total height of the die is reduced to fit between the electrodes. Please click here to view a larger version of this figure.

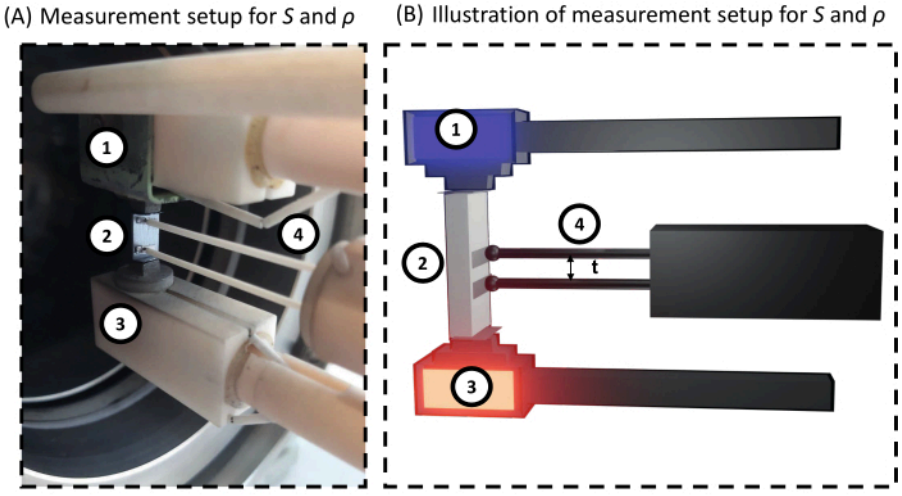

Figure 3: Measurement setup of the electrical conductivity and the Seebeck coefficient. For both (**A**) realistic view of the bar loaded into the device and (**B**) schematic view; 1) electrode, 2) sample, 3) electrode with gradient heater, and 4) thermocouples/ probes. Between the sample and the electrodes and thermocouples are thin pieces of graphite, aiding the preservation of the device. Please click here to view a larger version of this figure.

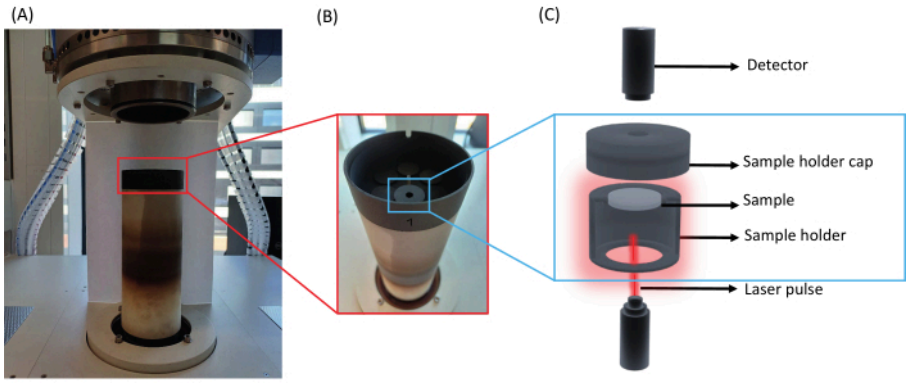

Figure 4: Thermal diffusivity measurement setup. (**A**) Open view of the analyzer, (**B**) enhanced view of the automated magazine with a sample inside, and (**C**) schematic illustration of a sample loaded inside a sample holder. Please click here to view a larger version of this figure.

Representative Results

The fabrication of SnSe particles relies on the complete dissolution of the precursors in their stoichiometric ratios. An essential step in the protocol involves the reduction of Se with $NaBH_4$, while under inert conditions. Any slight exposure to air results in the Se precursor changing from colorless to red (formation of polyselenides), as demonstrated in **Figure 5**.

Following the synthesis of SnSe, the particles are subjected to a purification procedure. The first supernatant of the purification process is yellow but upon exposure to oxygen turns orange. This is the result of unreacted Se, as the precursor was added in excess. In addition, there is a loss of small particles as shown in **Figure 6** (steps #3 and onwards). At high ionic strength, the surface charge of the particles is efficiently shielded, allowing particles to be closer together without experiencing repulsion. With every washing step, the ionic strength decreases and the particle surface is not shielded; thus, particles repel and remain colloidally stable and consequently, are lost during the purification procedure.

The synthesis of SnSe yields ~14 g per batch of pure phase SnSe, as confirmed by XRD (**Figure 7A**). The particles are polydisperse in shape with a size between 50 nm and 200 nm (**Figure 7B**). After annealing, the average size of the particles increases to 680 nm. The densification using SPS also promotes grain growth, and the resulting pellets have a relative density of >90%. A comparison of grain size is done from the SEM images between the untreated SnSe and SnSe-CdSe nanocomposite (**Figure 7B** and **Figure 7C**, respectively). Following the surface treatment results in grains that are considerably smaller compared to the untreated SnSe.

The cut and polished samples are then postannealed to confer stability. The, σ, S, and αare measured using the setups in **Figure 3** and **Figure 4**, respectively. From the measurements, the κ and zT are calculated with error bars

calculated considering the propagation of uncertainties from each measurement (**Figure 8**).

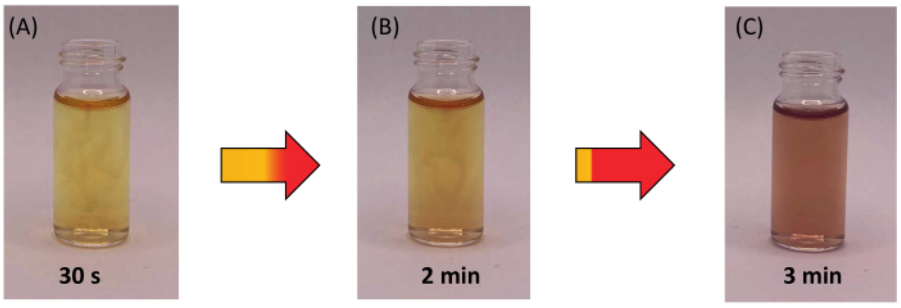

Figure 5: Time lapse of Se precursor on exposure to air. (**A**) Instant exposure to air results in a yellow solution. (**B**) After 2 min, the solution begins to turn red, and (**C**) within 3 min, the solution turns reddish as a result of Se oxidation. Please click here to view a larger version of this figure.

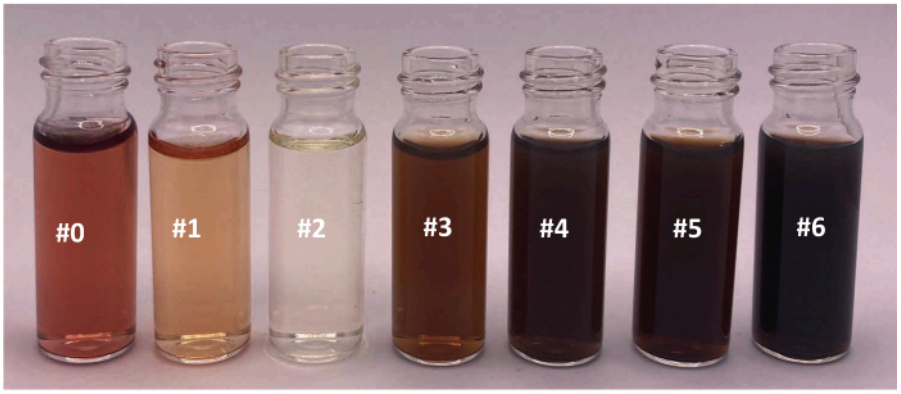

Figure 6: Supernatants after each washing step in the purification of SnSe. The colors of the seven supernatants of the different washing steps. Please click here to view a larger version of this figure.

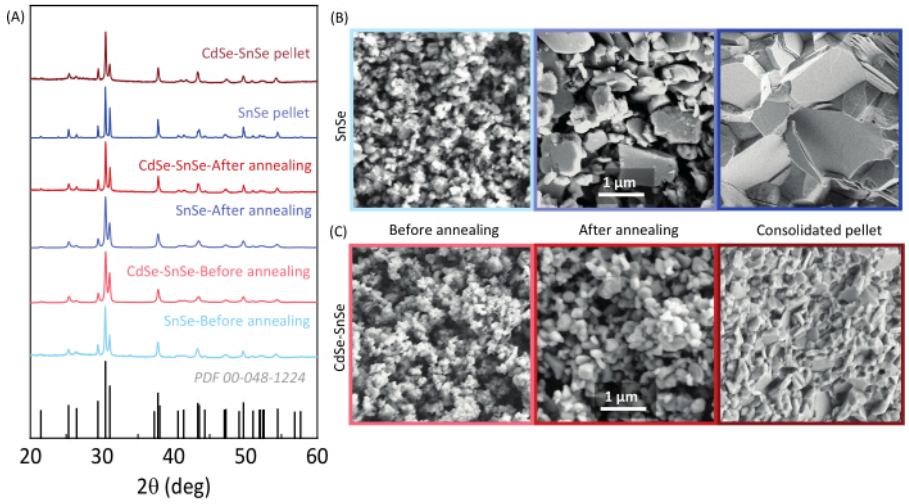

Figure 7: Structural and morphological analysis of the SnSe and CdSe-SnSe particles and pellet. (**A**) XRD analysis and SEM images of (**B**) SnSe and (**C**) CdSe-SnSe particles obtained after the solution synthesis, annealed powder, and consolidated pellet. Scale bars = 1 μm. This figure has been modified from Liu et al.[22]. Please click here to view a larger version of this figure.

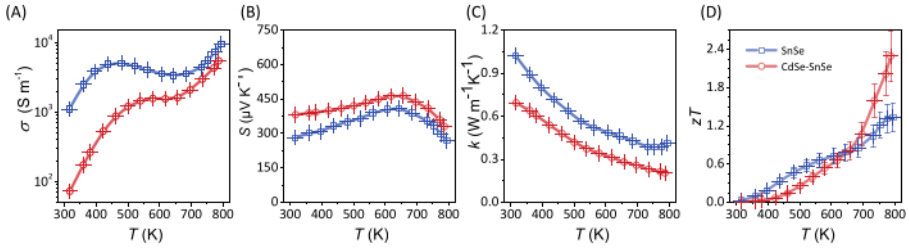

Figure 8: Thermoelectric properties of pure SnSe and CdSe-SnSe. (**A**) Electrical conductivity, (**B**) Seebeck coefficient, (**C**) total thermal conductivity, and (**D**) thermoelectric figure of merit. Please click here to view a larger version of this figure.

Supplemental Figure S1: Die characteristics and dimensions. Please click here to download this File.

Supplemental Figure S2: Adapters used to cut the SnSe samples with respect to the pressing directions. Please click here to download this File.

Supplemental Figure S3: Density measurement setup for SnSe and CdSe-SnSe samples. The mass of the pellet measured in (**A**) air and (**B**) water. Please click here to download this File.

Supplemental Table S1: Die characteristics and specifications. Please click here to download this File.

Discussion

Critical steps

Selenium oxidation before mixing with the Sn precursor

In this work, SnSe is synthesized by co-precipitation of Sn (II) complexes and Se^{2-}. We start by reducing metallic selenium to selenide.

$$Se^{0}_{(s)} + 2\,e^{-} \xrightarrow{NaBH_{4(aq)}} Se^{2-}_{(aq)}$$

Once the selenium (grey) is reduced, it forms a transparent solution. The selenium precursor, once exposed to oxygen, turns red, due to the formation of polyselenides. Thus, it is important to keep all solutions under argon for the duration of the reaction.

$$n\,Se^{2-}_{(aq)} \xrightarrow{O_{2(aq-air)}} Se^{2-}_{n} + (2n-2)\,e^{-}$$

On heating the tin chloride and sodium hydroxide, the tin precursor dissolves into a colorless solution as well.

$$SnCl_2 \cdot 2H_2O_{(s)} \xrightarrow{NaOH_{(aq)}} Sn(OH)^{2-}_{4\ (aq)}$$

Upon addition of the selenide, which is in excess (0.9:1; Sn:Se), to the tin precursor, the mixture turns black, indicating the immediate formation of SnSe.

$$Se^{2-}_{(aq)} + Sn^{2+}_{(aq,various\ species)} \longrightarrow SnSe_{(s)}$$

As small amounts of the $NaBH_4$ reagent react with the water, it is important to prevent oxidation of the Se by adding an excess of NaBH4[23,24,25]. Even though the formation of SnSe is instantaneous, the reaction is kept at ~100 °C for a further 2 h to allow the particles to grow[26,27].

Purification

The as-synthesized particles are then subjected to a purification procedure since they are in suspension with byproducts such as Na^{+}, Cl^{-}, $B(OH)_3$, $B(OH)_4^{-}$, OH^{-}, and excess BH_4^{-} and Se^{2-}/HSe^{-} and potential impurities. This is carried out for six purification steps of alternating water and ethanol as solvents[28,29,30,31,32,33,34,35]. Deviation in the purification procedure results in pellets with different performances, while the structural characterization looks identical.

Preparing CdSe thiol-amine solution fresh

CdSe molecular complexes are stable for a limited period in the thiol-amine solution and therefore, should be used within 24 h after the dissolution is completed[22].

Vacuum drying

Vacuum drying creates a lower-pressure environment, which facilitates the rapid removal of solvents from the particles. This is essential to prevent the formation of residual solvent pockets within the particles, which can negatively affect the sintering process and the final pellet properties or stability.

Annealing powders after purification in a reducing atmosphere

Annealing the particles is important to remove any prevalent volatile impurities, for example, thiol, amine, and excess Se[36,37,38]. Oxygen exposure of the particles is inevitable and thus, annealing in a reducing atmosphere aids in the reduction of oxides that inherently enhance the thermal conductivity of the material[39,40,41].

Evaluate performance in two directions, parallel and perpendicular

In accordance with the anisotropic nature of SnSe, electrical and thermal transport properties are different in

the pressing (parallel) and non-pressing (perpendicular) directions. Therefore, it is important to prepare cylindrical pellets with dimensions that allow for the cutting of a bar and a disk to measure the transport properties in both directions[41].

Sample preparation for transport characterization

A smooth and flat pellet surface is crucial for accurate diffusivity measurements. Imperfections on the pellet surface can lead to heat losses and inaccurate results. Polishing is necessary to achieve a uniform and smooth surface. The orientation of the treated and untreated SnSe when loading is important and crucial for correct transport data analysis. Anisotropic materials such as SnSe must be measured along the same direction and combined (σ, S, and κ) for an accurate zT. Proper thermal contacts between the pellet and probes are also critical for accurate S and ρ measurements.

Limitations

However, due to the use of sodium reagents, the method is limited to producing *p*-type SnSe as Na^+ ions are adsorbed onto the surface of the particles and act as a dopant enhancing the carrier concentration and σ of the material[42].

Significance of the technique with respect to existing/ alternative methods

Various solution-based techniques have been reported to prepare polycrystalline SnSe such as solvothermal, hydrothermal, and non-pressurized methods in water or ethylene glycol[18,19]. In this work, we focused on a surfactant-free aqueous synthesis[43], as it is more sustainable than any other reported methods: no organic solvents nor surfactants are used, and it requires a short reaction time (2 h) and low temperatures (~100 °C) compared to those done by melting.

Future applications or directions after mastering this technique

The method is adaptable in synthesizing other chalcogenides-SnTe, PbSe, and PbTe. In amending the reducing agents and bases to Na-free, pure materials without an intentional dopant can be synthesized. Surface treatments, such as the one done here with CdSe molecular complexes, allow for an added degree of flexibility in the material preparation, where secondary phases can be added in a secondary step to control the microstructure. In the specific case described here, the presence of CdSe nanoparticles not only inhibits the grain growth of the CdSe-SnSe particles compared to that of SnSe, but also lowers the thermal conductivity of the material (**Figure 7** and **Figure 8**, respectively). Explanations that have been reported by Liu et al. [22] support the results postulated from the method we have stipulated in this work.

Disclosures

The authors have no conflicts of interest to declare.

Acknowledgments

The Scientific Service Units (SSU) of ISTA supported this research through resources provided by the Electron Microscopy Facility (EMF) and the Lab Support Facility (LSF). This work was financially supported by the Institute of Science and Technology Austria and the Werner Siemens Foundation.

References

1. Alam, H., Ramakrishna, S. A review on the enhancement of figure of merit from bulk to nano-thermoelectric materials. *Nano Energy.* **2** (2) 190-212 (2013).
2. Ortega, S. et al. Bottom-up engineering of thermoelectric nanomaterials and devices from solution-processed

nanoparticle building blocks. *Chemical Society Reviews.* **46** (12), 3510-3528 (2017).

3. Tan, G., Zhao, L. D., Kanatzidis, M. G. Rationally designing high-performance bulk thermoelectric materials. *Chemical Reviews.* **116** (19), 12123-12149 (2016).
4. Ibáñez, M. et al. High-performance thermoelectric nanocomposites from nanocrystal building blocks. *Nature Communications.* 7, 10766 (2016).
5. Liu, Y., Ibáñez, M. Tidying up the mess. *Science.*, **371** (6530), 678-679 (2021).
6. Zhao, L. D. et al. Ultralow thermal conductivity and high thermoelectric figure of merit in SnSe crystals. *Nature.* **508** (7496), 373-377 (2014).
7. Chang, C. et al. 3D charge and 2D phonon transports leading to high out-of-plane ZT in n-type SnSe crystals. *Science.* **360** (6390), 778-783 (2018).
8. Lee, Y. K., Luo, Z., Cho, S. P., Kanatzidis, M. G., Chung, I. Surface oxide removal for polycrystalline SnSe reveals near-single-crystal Thermoelectric Performance. *Joule.* **3** (3), 719-731 (2019).
9. Lee, Y. K. et al. Enhancing p-type thermoelectric performances of polycrystalline SnSe via tuning phase transition temperature. *Journal of the American Chemical Society.*, **139** (31), 10887-10896 (2017).
10. Zhou, C. et al. Polycrystalline SnSe with a thermoelectric figure of merit greater than the single crystal. *Nature Materials.* **20** (10), 1378-1384 (2021).
11. Caballero-Calero, O., Ares, J. R., Martín-González, M. Environmentally friendly thermoelectric materials: high performance from inorganic components with low toxicity and abundance in the earth. *Advanced Sustainable Systems.* **5** (11), 2100095 (2021).
12. Guélou, G., Powell, A. V., Vaqueiro, P. Ball milling as an effective route for the preparation of doped bornite: Synthesis, stability and thermoelectric properties. *Journal of Materials Chemistry C.* **3** (40), 10624-10629 (2015).
13. Chen, X. et al. Preparation of nano-sized Bi2Te3 thermoelectric material powders by cryogenic grinding. *Progress in Natural Science: Materials International.* **22** (3), 201-206 (2012).
14. Zhang, S. N. et al. Effects of ball-milling atmosphere on the thermoelectric properties of TAGS-85 compounds. *Journal of Electronic Materials.* **38** (7), 1142-1147 (2009).
15. Bumrungpon, M. et al. Synthesis and thermoelectric properties of bismuth antimony telluride thermoelectric materials fabricated at various ball-milling speeds with yttria-stabilized zirconia ceramic vessel and balls. *Ceramics International.* **46** (9), 13869-13876 (2020).
16. Zevalkink, A. et al. A practical field guide to thermoelectrics: Fundamentals, synthesis, and characterization. *Applied Physics Reviews.*, **5** (2), 021303 (2018).
17. Chandra, S., Biswas, K. Realization of high thermoelectric figure of merit in solution synthesized 2D SnSe nanoplates via Ge alloying. *Journal of the American Chemical Society.* **141** (15), 6141-6145 (2019).
18. Shi, X.; Tao, X.; Zou, J.; Chen, Z. High-performance thermoelectric SnSe: aqueous synthesis, innovations, and challenges. *Advanced Science*. **7** (7), 1902923 (2020).

19. Shi, X. L. et al. A solvothermal synthetic environmental design for high-performance SnSe-based thermoelectric materials. *Advanced Energy Materials.* **12** (20), 1-10 (2022).
20. Liu, Y. Lee, S. Fiedler, C. Spadaro, M.C. Chang, C. Li, M. Hong, M. Arbiol, J. Ibáñez, M. Enhancing thermoelectric performance of solution-processed polycrystalline SnSe with PbSe nanocrystals. *Chemical Engineering Journal.* **490** (2024).
21. Fiedler, C. Calcabrini, M. Liu, Y. Ibáñez, M. Unveiling Crucial Chemical Processing Parameters Influencing the Performance of Solution-processed inorganic Thermoelectric Materials. *Angewandte Chemie International edition.* (2024).
22. Liu, Y. et al. Defect engineering in solution-processed polycrystalline SnSe leads to high thermoelectric performance. *ACS Nano.* **16** (1), 78-88 (2022).
23. Lalancette, J. M.; Arnac, M. Reductions with sulfurated borohydrides. III. Borohydrides incorporating selenium and tellurium. *Canadian Journal of Chemistry.* **47** (19), 3695-3697 (1969).
24. Klayman, D. L.; Griffin, T. S. Reaction of selenium with sodium borohydride in protic solvents. A facile method for the introduction of selenium into organic molecules. *Journal of the American Chemical Society.* **95** (1), 197-199 (1973).
25. Goldbach, A.; Saboungi, M. L.; Johnson, J. A.; Cook, A. R.; Meisel, D. Oxidation of aqueous polyselenide solutions. A mechanistic pulse radiolysis study. *The Journal of Physical Chemistry A.* **104** (17), 4011-4016 (2000).
26. Yarema, M. et al. Upscaling colloidal nanocrystal hot-injection syntheses via reactor underpressure. *Chemistry of Materials.* **29** (2), 796-803 (2017).
27. Kwon, S. G., Hyeon, T. Formation mechanisms of uniform nanocrystals via hot-injection and heat-up methods. *Small.* **7** (19), 2685-2702 (2011).
28. Han, G. et al. Topotactic anion-exchange in thermoelectric nanostructured layered tin chalcogenides with reduced selenium content. *Chemical Science.* **9** (15), 3828-3836 (2018).
29. Tang, G. et al. Realizing high figure of merit in phase-separated polycrystalline Sn1-XPbxSe. *Journal of the American Chemical Society.* **138** (41), 13647-13654 (2016).
30. Sirikumara, H. I., Morshed, M., Jameson, C., Jayasekera, T. Dopant-induced indirect-direct transition and semiconductor-semimetal transition of bilayer SnSe. *Journal of Applied Physics.* **126** (22), 224301 (2019).
31. Zhang, Q. K. et al. Enhanced thermoelectric performance of a simple method prepared polycrystalline SnSe optimized by spark plasma sintering. *Journal of Applied Physics.* **125** (22), 225109 (2019).
32. Shi, X. et al. Boosting the thermoelectric performance of P-type heavily Cu-doped polycrystalline SnSe via inducing intensive crystal imperfections and defect phonon scattering. *Chemical Science.* **9** (37), 7376-7389 (2018).
33. Xu, R. et al. Nanostructured SnSe integrated with Se quantum dots with ultrahigh power factor and thermoelectric performance from magnetic field-assisted hydrothermal synthesis. *Journal of Materials Chemistry A.* **7** (26), 15757-15765 (2019).

34. Shi, X. et al. High thermoelectric performance in P-type polycrystalline Cd-doped SnSe achieved by a combination of cation vacancies and localized lattice engineering. *Advanced Energy Materials.* **9** (11), 1803242 (2019).
35. Li, M. et al. Crystallographically textured SnSe nanomaterials produced from the liquid phase sintering of nanocrystals. *Dalton Transactions.* **48** (11), 3641-3647 (2019).
36. Cargnello, M. et al. Efficient removal of organic ligands from supported nanocrystals by fast thermal annealing enables catalytic studies on well-defined active phases. *Journal of the American Chemical Society.* **137** (21), 6906-6911 (2015).
37. Mohapatra, P. et al. Calcination does not remove all carbon from colloidal nanocrystal assemblies. *Nature Communications.* **8** (1), 2038 (2017).
38. Ibáñez, M. et al. Electron doping in bottom-up engineered thermoelectric nanomaterials through HCl-mediated ligand displacement. *Journal of the American Chemical Society.* **137** (12), 4046-4049 (2015).
39. Chen, Y. X. et al. Understanding of the extremely low thermal conductivity in high-performance polycrystalline SnSe through potassium doping. *Advanced Functional Materials.* **26** (37), 6836-6845 (2016).
40. Zhao, L. D.; Chang, C.; Tan, G.; Kanatzidis, M. G. *SnSe:* A remarkable new thermoelectric material. *Royal Society of Chemistry.* **9**, 3044-3060 (2016).
41. Wei, T.-R. et al. How to measure thermoelectric properties reliably. *Joule.* **2**(11), 2183-2188 (2018).
42. Liu, Y. et al. The importance of surface adsorbates in solution-processed thermoelectric materials: The case of SnSe. *Advanced Materials.* **33** (52), 2106858 (2021).
43. Han, G. et al. Facile surfactant-free synthesis of p-type SnSe nanoplates with exceptional thermoelectric power factors. *Angewandte Chemie.* **128** (22), 6543-6547 (2016).